Generic formulation of a generalized Lorenz-Mie theory for pulsed laser illumination.

By

G. Gouesbet, L. Mees, and G. Gréhan

Laboratoire d'Energétique des Systèmes et Procédés,
Unité Mixte de Recherche 6614/CORIA
CNRS/INSA et Université de Rouen,
BP 08,
76 131 Mont Saint Aignan, France

ABSTRACT

During the two last decades, a vigorous effort has been devoted to the study of interactions between arbitrary shaped beams (for continuous waves) and particles. When the particle under study allows one to solve the scattering problem by relying on the separability of variables, we say that the associated theory is a generalized Lorenz-Mie theory (GLMT). At the present time, GLMTs are available for the following king of particles: homogeneous spheres, multilayered spheres, ellipsoids, infinitely long cylinders (with circular or elliptical cross-sections), sphere with one arbitrarily located spherical inclusion, and aggregates. Such a theories are relevant to the field of optical particle characterization in two-phase flows (phase-Doppler systems, rainbow refractometry, shadow Doppler techniques, for instance).

The aforementioned GLMTs are extensions of simpler theories when particles are illuminated by continuous plane waves. Another line of extension is by considering the case of illumination by pulses (single pulses or train of pulses), viewed as continuous arbitrary shaped beams modulated by a pulse envelope.

Nowadays, pulsed laser beams become of common use, with a growing interest for the generation and applications of femtosecond pulses. In particular, pulsed lasers may activate many interesting nonlinear phenomena in microcavities, such as stimulated Raman scattering, stimulated Brillouin scattering, third-order sum generation or lasing. They open the way for new optical particle characterization techniques, for instance concerning measurements of chemical species concentration in droplets.

It is therefore desirable to possess a GLMT for the case of particles illuminated by laser pulses, with arbitrary spatial supports. Such a GLMT will be presented in this paper. This GLMT is said to be generic. The word "generic" means that the theory is presented under a form allowing one to consider arbitrary scattering particles.

1. INTRODUCTION

During the two last decades, a vigorous effort has been devoted to the study of interactions between arbitrary shaped beams (for continuous waves) and particles. When the particle under study allows one to solve the scattering problem by relying on the separability of variables, we say that the associated theory is a generalized Lorenz-Mie theory (GLMT). At the present time, GLMTs are available for the following king of particles: homogeneous spheres, multilayered spheres, ellipsoids, infinitely long cylinders (with circular or elliptical cross-sections), sphere with one arbitrarily located spherical inclusion, and aggregates. Such a theories are relevant to the field of optical particle characterization in two-phase flows (phase-Doppler systems, rainbow refractometry, shadow Doppler techniques, for instance)[1, 2, 3].

The aforementioned GLMTs are extensions of simpler theories when particles are illuminated by continuous plane waves. Another line of extension is by considering the case of illumination by pulses (single pulses or train of pulses), viewed as continuous arbitrary shaped beams modulated by a pulse envelope.

Nowadays, pulsed laser beams become of common use, with a growing interest for the generation and applications of femtosecond pulses. In particular, pulsed lasers may activate many interesting nonlinear phenomena in microcavities, such as stimulated Raman scattering, stimulated Brillouin scattering, third-order sum generation or lasing. They open the way for new optical particle characterization techniques, for instance concerning measurements of chemical species concentration in droplets.

It is therefore desirable to possess a GLMT for the case of particles illuminated by laser pulses, with arbitrary spatial supports. Such a GLMT will be presented in this paper. This GLMT is said to be generic. The word "generic" means that the theory is presented under a form allowing one to consider arbitrary scattering particles.

The paper is organized as follows. Section 2 presents the general formulation and is a summary of a material developed in [4]. Also, section 3 considers the case of a Rayleigh dipole allowing one to present an analytical discussion of the formulation. Section 4 discusses the more realistic case of a sphere illuminated by a pulsed Gaussian beam (Gaussian envelope), with plane wave or Gaussian spatial supports. Section 5 is a conclusion.

2. GENERAL FORMULATION.

We consider a pulsed electromagnetic wave of the form:

$$X_i(r,\boldsymbol{t}) = X_0 X_i^s(r)\exp(2i\boldsymbol{pn}_0\boldsymbol{t})g(\boldsymbol{t}) \tag{1}$$

in which X designates either E (electric field) or H (magnetic field), i is a component subscript (in a coordinate system matching the shape of the particle), r is a point in space, $X_i^s(r)$ describes the laser shape and is called the spatial support of the pulse, ν_0 is the carrier frequency, $g(\tau)$ is the (real) pulse envelope and τ is a shifted time:

$$\boldsymbol{t} = t - z/c \tag{2}$$

in which t is the time, z the axis of propagation of the beam, and c the speed of light. This formulation is quite general and is obtained by multiplying the general description of a continuous wave laser beam [5] by the pulse envelope $g(\tau)$. The pulse propagates in a transparent medium and, for convenience in this paper, $g(\tau)$ represents an unique pulse (not a train of pulses).

We assume that we are allowed to introduce a pair of Fourier transforms reading as:

$$G(\boldsymbol{n}) = \int_{-\infty}^{+\infty} g(\boldsymbol{t}) \exp(-2i\boldsymbol{pnt}) d\boldsymbol{t} \tag{3}$$

$$g(\boldsymbol{t}) = \int_{-\infty}^{+\infty} G(\boldsymbol{n}) \exp(+2i\boldsymbol{pnt}) d\boldsymbol{n} \tag{4}$$

where G(ν) is the pulse envelope spectrum. Conditions of existence for the pair are not discussed here, but, in general, the Fourier transform should be interpreted in terms of mathematical distributions [6, 7] (see next section). The envelope g(τ) being real, its spectrum is Hermitian:

$$G(\boldsymbol{n}) = G(-\boldsymbol{n})^* \tag{5}$$

leading to:

$$g(\boldsymbol{t}) = \int_{0}^{+\infty} G(\boldsymbol{n}) \exp(+2i\boldsymbol{pnt}) d\boldsymbol{n} + \int_{0}^{+\infty} G(\boldsymbol{n})^* \exp(-2i\boldsymbol{pnt}) d\boldsymbol{n} \tag{6}$$

From Eqs (1) and (6):

$$X_i(r,\boldsymbol{t}) = X_0 X_i^s(r) \left[\int_{0}^{+\infty} G(\boldsymbol{n} - \boldsymbol{n}_0) \exp(+2i\boldsymbol{pnt}) d\boldsymbol{n} + \int_{0}^{+\infty} G(\boldsymbol{n} + \boldsymbol{n}_0)^* \exp(+2i\boldsymbol{pnt}) d\boldsymbol{n} \right] \tag{7}$$

showing that the pulsed illumination can be decomposed into an integral of elementary monochromatic waves. The response to each monochromatic wave is assumed to be known (for instance, use a continuous wave GLMT). The response of the scatterer to an excitation $X_0 X_i^S(r) \exp(\pm 2i\boldsymbol{pnt})$ then reads as $X_i^{cw}(r, \pm \boldsymbol{n}) \exp(\pm 2i\boldsymbol{pnt})$. This response of the scatterer to a pulse then is:

$$X_i^p(r,\boldsymbol{t}) = \left[\int_{0}^{+\infty} G(\boldsymbol{n} - \boldsymbol{n}_0) X_i^{cw}(r,\boldsymbol{n}) \exp(2i\boldsymbol{pnt}) d\boldsymbol{n} \right] + \tag{8}$$
$$\left[\int_{0}^{+\infty} G(\boldsymbol{n} + \boldsymbol{n}_0)^* X_i^{cw}(r,-\boldsymbol{n}) \exp(+2i\boldsymbol{pnt}) d\boldsymbol{n} \right]$$

From Hermiticity equation(5), Eq (8) becomes:

$$X_i^p(r,\boldsymbol{t}) = \widetilde{F}^{-1} \left[G(\boldsymbol{n} - \boldsymbol{n}_0) X_i^{cw}(r,\boldsymbol{n}) \right] \tag{9}$$

in which $\widetilde{F}^{-1}$ designates an inverse Fourier transform and the tilde means that the variable conjugated with (is the time t (not the shifted time τ).

RAYLEIGH DIPOLE

To illustrate the formulation, we first consider a case which can be analytically solved. Let us consider a Rayleigh dipole illuminated by a pulse with a plane wave spatial support, propagating along z, with the electric field oscillating parallely to x. Eq (1) becomes:

$$E_1 = E_0 \exp(2i\boldsymbol{pnt}) g(\boldsymbol{t}) \tag{10}$$

and we take an envelope:

Figure 1 : Representation of the pulse envelope, at time t=0.

$$g(\boldsymbol{t}) = \prod\left(\frac{\boldsymbol{t} - L/\boldsymbol{n}_0}{M/\boldsymbol{n}_0}\right) \qquad\qquad , \text{L,M} > 0, \ \text{L>M/2} \qquad\qquad (11)$$

displayed in Fig 1, for t=0. A Rayleigh dipole is located at z=0. The pulse excitation reaches the dipole at t=(L-M/2)λ_0/c and leaves it at t=(L+M/2)λ_0/c. We establish:

$$\prod\left(\frac{\boldsymbol{t} - L/\boldsymbol{n}_0}{M/\boldsymbol{n}_0}\right) = \frac{M}{\boldsymbol{n}_0}\prod\left(\frac{\boldsymbol{t}}{M/\boldsymbol{n}_0}\right) * \boldsymbol{d}(\boldsymbol{t} - L/\boldsymbol{n}_0) \qquad\qquad (12)$$

in which (is the Dirac distribution and (*) designates a convolution product. Using:

$$\mathbf{F}[\text{S*T}] = \mathbf{F}[\text{S}] \text{ x } \mathbf{F}[\text{T}] \qquad\qquad (13)$$

in which S and T are distributions and, $\mathbf{F}$ is a direct Fourier transform, we have:

$$G(\boldsymbol{n}) = \frac{M}{\boldsymbol{n}_0}\frac{\sin \boldsymbol{p}\boldsymbol{n}M/\boldsymbol{n}_0}{\boldsymbol{p}\boldsymbol{n}}\exp(-2i\boldsymbol{p}\boldsymbol{n}L/\boldsymbol{n}_0) \qquad\qquad (14)$$

The response of a Rayleigh dipole to an excitation $E_0\exp(2i\boldsymbol{p}\boldsymbol{n}_0\boldsymbol{t})$, for a scattered electric field oscillating along x, propagating toward positive z's, with a constant complex refractive index reads as [8]:

$$E_0\frac{K}{z}\boldsymbol{n}^2\exp(2i\boldsymbol{p}\boldsymbol{n}\boldsymbol{t})\exp(2i\boldsymbol{p}\boldsymbol{n}z/c) \qquad\qquad (15)$$

in which K is a constant.

Using Eqs (9) and (14), we afterward establish:

$$E_1^p(z,t) = E_0 \frac{KM}{z \boldsymbol{n}_0} \tilde{F}^{-1}\left[\boldsymbol{n}^2\right] * \tilde{F}^{-1}\left[\exp(2i\boldsymbol{p}\boldsymbol{n}z/c)\right] \tag{16}$$

$$* \tilde{F}^{-1}\left[\frac{\sin \boldsymbol{p}(\boldsymbol{n}-\boldsymbol{n}_0)M/\boldsymbol{n}_0}{\boldsymbol{p}(\boldsymbol{n}-\boldsymbol{n}_0)}\exp(-2i\boldsymbol{p}(\boldsymbol{n}-\boldsymbol{n}_0)L/\boldsymbol{n}_0)\right]$$

We evaluate separately each inverse Fourier transform, in particular:

$$\tilde{F}^{-1}\left[\boldsymbol{n}^2\right] = -\frac{\boldsymbol{d}''(t)}{4\boldsymbol{p}^2} \tag{17}$$

and use:

$$\boldsymbol{d}'' * T = T'' \tag{18}$$

to establish:

$$E_1^p(z,t) = -\frac{K}{4\boldsymbol{p}^2}\frac{E_0\boldsymbol{n}_0}{zM}\frac{d^2}{dt^2}\left[\prod\left(\frac{t-z/c-L/\boldsymbol{n}_0}{M/\boldsymbol{n}_0}\right)\exp(2i\boldsymbol{p}\boldsymbol{n}_0(t-z/c))\right] \tag{19}$$

The second derivative is evaluated with the following ingredients:

1. the derivative of a convolution product of two distributions is obtained by only deriving one distribution.

2. We have:

$$\prod(x) = H(x+1/2) - H(x-1/2) \tag{20}$$

in which **H** is the Heaviside distribution.

3. We have:

$$H'(x) = \boldsymbol{d}(x) \tag{21}$$

We then obtain:

$$E_1^p(z,t) = -\frac{KE_0}{4\boldsymbol{p}^2 z}\left\{-\frac{4\boldsymbol{p}^2\boldsymbol{n}_0^3}{M}\prod\left(\frac{t-z/c-L/\boldsymbol{n}_0}{M/\boldsymbol{n}_0}\right)\exp(i2\boldsymbol{p}\boldsymbol{n}_0(t-z/c))\right\} + \tag{22}$$

$$\text{Dirac singularit ies}$$

The singularities (full expression not given), depending on δ and δ', occur at times when the scattered pulse reaches and leaves the location z>0. Since a Rayleigh dipole has no inertia, we then see that the causality principle is

satisfied, illustrating the coherence of the formulation.

3. FINITE SPHERE

We now consider a more realistic case, requiring the use of numerical evaluations.

3.1 Configuration under study

The configuration under study is displayed in Fig 2. A pulsed laser beam, with a Gaussian spatial support characterized by its beam waist radius ω_0, its pulse time width Δt (full length at half-width) and its carrier wavelength λ_0, is scattered by a homogeneous spherical particle. The particle has a diameter d, a complex refractive index m=n-ik, and its location with respect to the beam waist center is (x_0, y_0, z_0). We aim to predict the properties of the scattered light in the direction defined by an angle (, in the far field domain).

The results are displayed as intensity versus a time delay. The time delay is defined as the time difference between the arrival time of the scattered light at the detector and the arrival time of a virtual ray which would travel, in free space, to the particle center and thereafter from the particle center to the detector. With such a definition of the time delay, we recover the classical geometrical optics formulation used in Phase Doppler anemometry [9, 10]. Optical path differences may also be evaluated as a time delay times the speed of light. As a consequence, reflected light, with an optical path smaller than the reference path, exhibits a positive time delay while, conversely, all the other scattering modes exhibit a negative time delay.

3.2 Exemplifying results, pulsed plane wave illumination.

We consider the case of a 100 µm particle diameter illuminated by a 100 fs pulse, with the center of the particle located at the beam waist center ($x_0 = y_0 = z_0 = 0$). The carrier wavelength of the illuminating beam is 0.6 µm. For convenience, we assume that the complex refractive index of the material does nor depend on the wavelength (remember that the pulse envelope generates a wavelength spectrum).
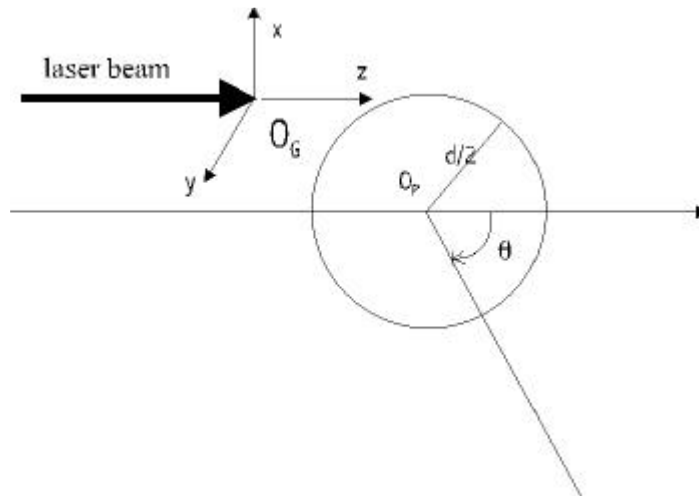

Figure 2 : The configuration under study, with the polarization defined by $\varphi = 0$
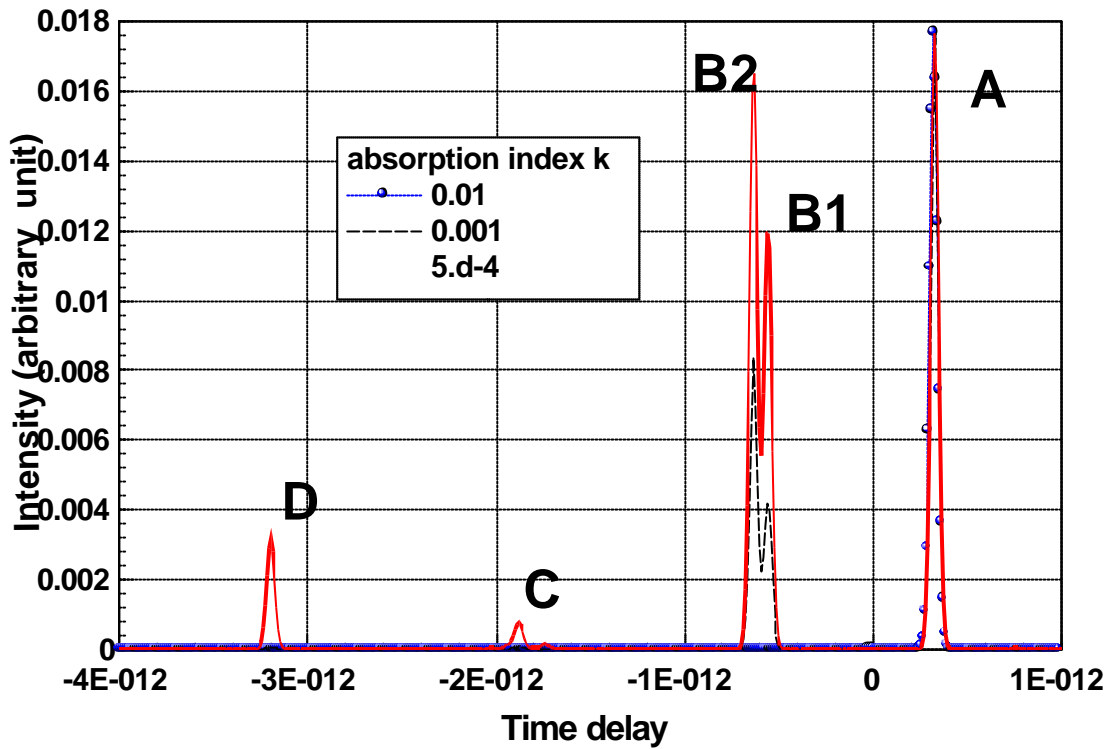
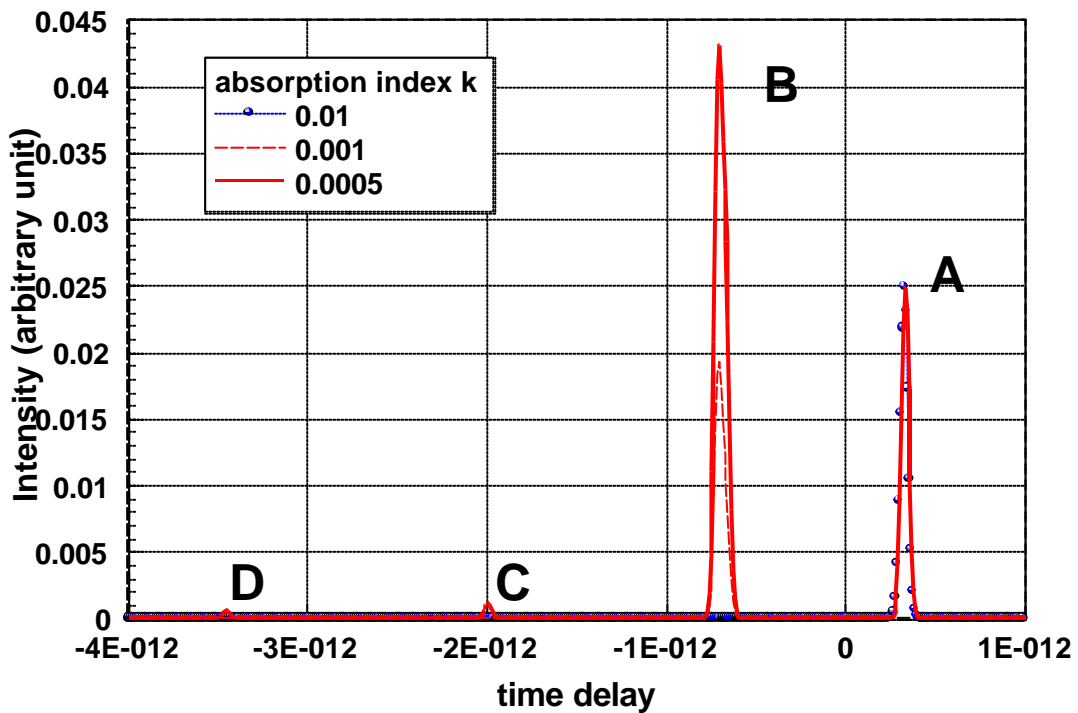Figure 3 : Pulsed plane wave backward scattering on a water droplet

Figure 4 : Pulsed plane wave backward scattering on a glass sphere.

Figures 3 and 4 display the light intensity scattered in backward direction,versus time delay, for particle with complex refractive indices m=1.33-ik and m=1.5-ik, with k as a parameter, respectively. The real parts of the indices are the ones for water and glass and, by extension, the materials will be designated as "water" and "glass"

respectively. Figure 5 displays the light intensity scattered in the direction θ=45°, versus time delay, for a water droplet, again with k as a parameter.
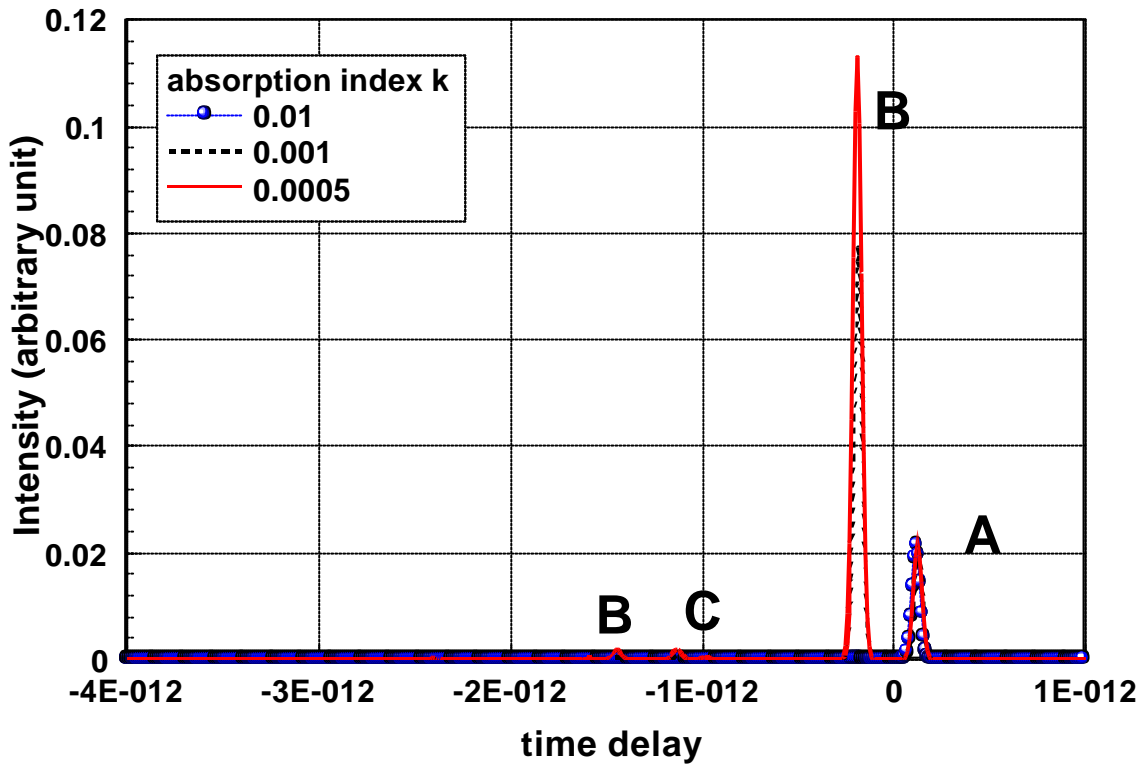

Figure 5 : Pulsed plane wave, 45° scattering on a water droplet.

All these curves exhibit a sequence of individual pulses in response to the illuminating single pulse. Indeed, during 100 fs, the light travels a distance which is about equal to 30 µm, i.e. about one third of the particle diameter. Therefore, elementary scattering responses (modes) which interfere together in the case of continuous wave illumination can be observed separately in the case of pulsed illumination.
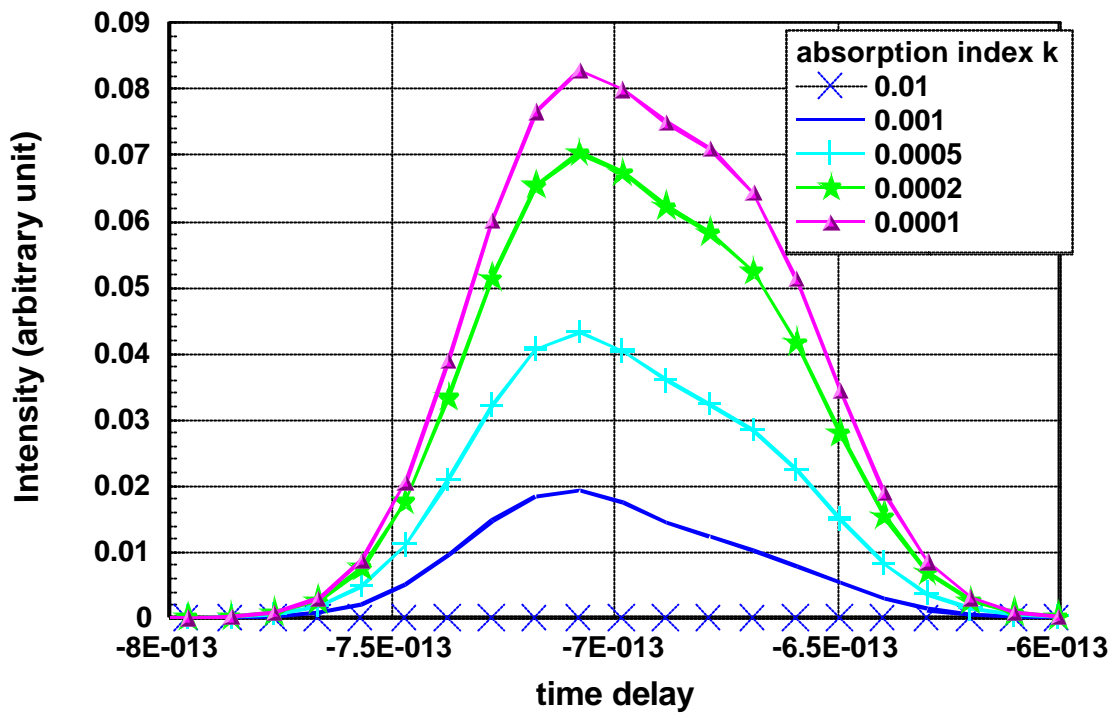
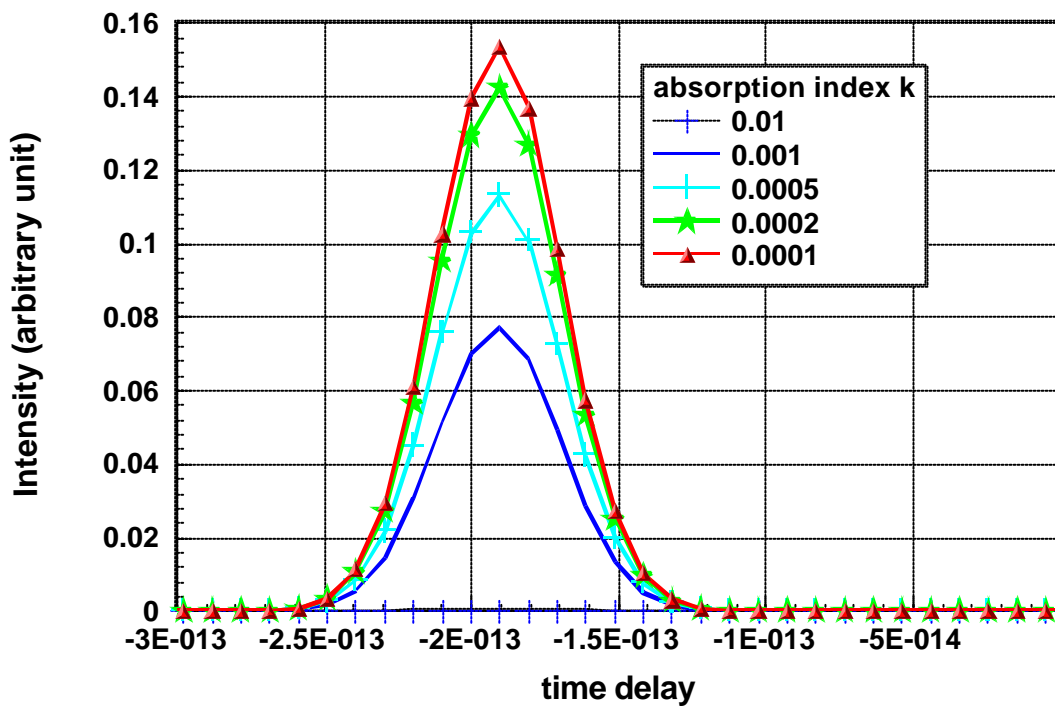Figure 6: Pulsed plane wave backward scattering on a glass sphere :
Details of peak B.

Figure 7: Pulsed plane wave, 45° scattering on a water droplet : details of peak B.

In Figure 3-5, there is only one peak, labelled A, exhibiting a positive time delay and which, therefore should be originating from a reflected light contribution. Accordingly, this peak does not depend on (in time delay) the refractive index of the material and, in particular, it does not depend on the imaginary part associated to the fact that the reflected light does not enter the particle. Also, we may quantitatively compare the time delays in Figs 3-5 for the

peaks labelled A with time delays evaluated with geometrical optics plain considerations, as displayed in Table 1, showing a very satisfactory agreement. Let us however note that there is a small residual difference in these comparisons. This residual is about equal to 5 fs (i.e. corresponding to about twice the wavelength duration). Our guess (unconfirmed) is that this residual might have a physical meaning and would possibly arise from the existence of evanescent waves near the outside boundary of the scatterer. A last fact is that a close examination of the peak A confirms that it has a Gaussian shape, with $\Delta t=100$ fs, corresponding to the illuminating pulse characterization.

	From figures	G.O. results
Water, 180°	327 fs	333 fs
Glass, 180°	327 fs	333 fs
Water, 45°	122 fs	127 fs

Table 1 : Comparaisons between pulsed GLMT
And geometrical optics predictions of
The time delay for reflected light contributions.

We next consider the first peak exhibiting a negative time delay, labelled B, in figs 3-5. Also, in Fig 3 for water, peak B is definitely bimodal, and the two modes are then labelled as B1 and B2. In complement, Figs 6 and 7 display an enlarged view of peak B plotted in Figs 4 and 5. In Fig 6 for glass, the peak B displays a fairly complex shape, which is reminiscent of a non resolved bimodal shape, with a width larger than 100 fs, indicating a complex behavior. Peak B is only essentially Gaussian versus time, with a width of about 100 fs (in agreement with the pulsed illumination duration), for the 45°-scattering on water (Figs 5 and 7). In this case, the geometrical optics time delay for refractive light (p=1 in van de Hulst notation) is -186 fs, i;e. very close to the time delay, equal to -190 fs, measured in Figs 5 or 7.

A tentative and partial discussion (albeit providing insights) to understand the complex behavior of peak B structures is now introduced. We then consider the behavior of rays which experience one internal reflection (p=2 in van de Hulst notation). In backward direction, for water, the ray with a zero impact parameter is the only one which exists. Conversely, for glass, there are two rays scattered in the backward direction, still one for zero impact parameter and the other one for an impact parameter close to 1 (edge ray). Associated time delays are -563 fs for water, and -666 fs, -708 fs for glass. These theoretical features are in agreement with peak B1 for water and (partially) with the shape of peak B for glass.

The existence of peak B2 for water however requires the use of considerations which do not pertain to geometrical optics, namely the introduction of surface waves which, in a naive but efficient picture, may by viewed as being associated with "photons" circulating around the particle, near the boundary surface. It is then reasonable to consider that the surface waves are circulating in an effective medium which has properties intermediary between the ones of water and the ones of the surrounding air. We therefore assume that this medium is characterized by an effective (real) refractive index. This index is evaluated in such a way that the ray experiencing two and half turn around the particle explains the location of peak D in Figs 3 and 4, leading to m=1.218 and m=1.3197 for water and glass respectively. Associated time delays are compiled in Table 2.

	measure	predicted	Turn(s)
Water, B2	- 634 fs	- 640 fs	0.5
Water, C	- 1882 fs	- 1914 fs	1.5
Water, D	- 3190 fs	- 3190 fs	2.5
Glass, B	- 701 fs	- 691 fs	0.5
Glass, C	- 1998 fs	- 2073 fs	1.5
Glass, D	- 3455 fs	- 3455 fs	2.5

Table 2: Comparisons between measured peak locations in Figs 3-4 and
"surface wave" predictions

We observe that our interpretation is in agreement with the existence of the peak B2 for water. This interpretation in terms of surface waves is also well supported by results obtained in the case of Gaussian (spatial support) pulsed illumination, in the framework of GLMT, as discussed in the last subsection. Let us also note that peak C location in Fig 5 with a time delay equal to -981 fs agrees with the geometrical optics calculation of the p=3 (again van de Hulst notation) scattered ray.

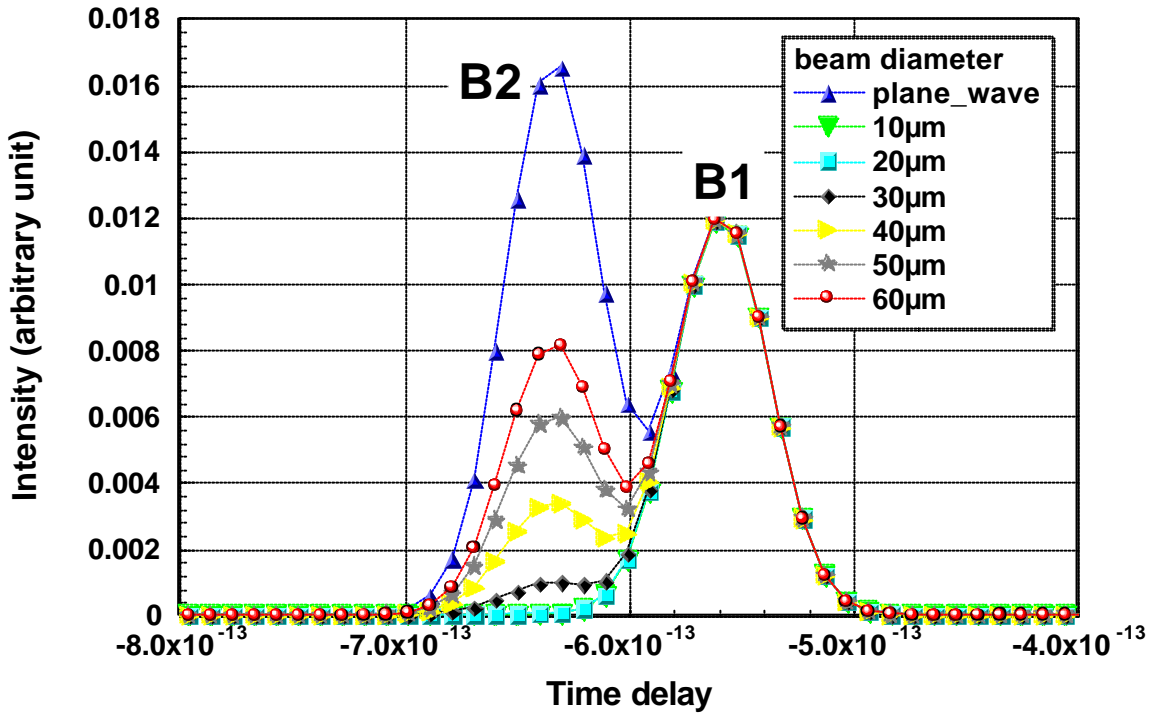**3.3 Gaussian (spatial support) beam illumination.**

Figure 8 : Backward water droplet scattering with the beam diameter
as parameter : details of peak B

We now replace the plane wave spatial support by a Gaussian spatial support, all other parameters being unchanged. results are plotted in Fig 8, zooming on peak B, with the beam diameter as a parameter. We observe that, if the Gaussian beam diameter is much smaller than the particle diameter (say $\omega_0 < 20$ µm), then only peak B1 is excited. increasing the beam diameter beyond, we observe an increasing excitation of the peak B2. These GLMT computations support our explanation of the existence of peak B2 in terms of surface waves.

4. CONCLUSION.

This paper presented a generic formulation of a GLMT describing the interaction between (arbitrary) scatterers and laser pulses. Exemplifying results are provided for rather large particles (diameter equal to 100 µm) and short pulses (100 fs), with plane wave and Gaussian spatial supports. Beside results well in agreements, our computations also demonstrate the ability of this GLMT to handle exotic phenomena such as surface waves. This new tool opens the way to many investigations, both theoretical and experimental, in the field of short pulse scattering.

REFERENCES

1. **G. Gouesbet and G. Gréhan**, *Generalized Lorenz-Mie theories, from past to future. Invited lecture to ICLASS 2000*, to be published in Atomization and Sprays.
2. **G. Gouesbet and G. Gréhan**, *Generalized Lorenz-Mie theory for a sphere with an*

eccentrically located spherical inclusion. To be published by J. Mod. Optics.

3. **G. Gouesbet and G. Gréhan** *Generalized Lorenz-Mie theory for assemblies of spheres and aggregates*. J. of Optics A: Pure and Applied Optics, 1:706--712, 1999.

4. **G. Gouesbet and G. Gréhan**. *Generic formulation of a generalized Lorenz-Mie theory for a particle illuminated by laser pulses*. Submitted to Applied Optics.

5. **G. Gouesbet**. *Exact description of arbitrary shaped beams for use in light scattering theories*. J. Opt. Soc. Am. A, 13(12):2434--2440, 1996.

6. **G.Gouesbet**. *Theory of distributions and its application to beam parametrization in light scattering*. Part. Part. Syst. Charact., 16:147--159, 1999.

7. **F. Roddier**. *Distributions et transformations de Fourier*. 1978. McGraw-Hill.

8. **L.P. Bayvel and A.R. Jones**. *Electromagnetic scattering and its applications*. 1981. Applied Science Publishers.

9. **R.W. Sellens**. *A derivation of phase Doppler measurement relation for an arbitrary geometry*. Experiments in Fluids, 8:165--168, 1989.

10. **H. Bultynck**. *Développement de sondes laser Doppler miniatures pour la mesure de particules dans des écoulements réels complexes*. PhD thesis, Université de Rouen, Fevrier 1998.